Letter

Energy dependent nuclear suppression from gluon saturation in exclusive vector meson production

Heikki Mäntysaari,[1,2,*] Farid Salazar,[3,4,5,6,7] and Björn Schenke[8]

[1]*Department of Physics, University of Jyväskylä, P.O. Box 35, 40014 University of Jyväskylä, Finland*
[2]*Helsinki Institute of Physics, P.O. Box 64, 00014 University of Helsinki, Finland*
[3]*Institute for Nuclear Theory, University of Washington, Seattle Washington 98195-1550, USA*
[4]*Nuclear Science Division, Lawrence Berkeley National Laboratory, Berkeley, California 94720, USA*
[5]*Physics Department, University of California, Berkeley, California 94720, USA*
[6]*Department of Physics and Astronomy, University of California, Los Angeles, California 90095, USA*
[7]*Mani L. Bhaumik Institute for Theoretical Physics, University of California, Los Angeles, California 90095, USA*
[8]*Physics Department, Brookhaven National Laboratory, Upton, New York 11973, USA*

(Received 20 December 2023; accepted 16 February 2024; published 15 April 2024)

We calculate exclusive J/ψ photoproduction at high energies in the color glass condensate approach. The results are compared to the center-of-mass energy dependent $\gamma + A \to J/\psi + A$ cross sections extracted from measurements in ultraperipheral heavy ion collisions at RHIC and LHC. We predict strong saturation-driven nuclear suppression at high energies, while LHC data prefer even stronger suppression. We explore effects of nucleon shaped fluctuations and show that the most recent measurement of the $|t|$-differential incoherent J/ψ cross section prefers large event-by-event fluctuations of the nucleon substructure in heavy nuclei, comparable to that found for a free proton.

DOI: 10.1103/PhysRevD.109.L071504

Introduction. Exclusive vector meson production in high-energy photon-nucleus collisions is a powerful tool to probe the nuclear wave function at a small longitudinal momentum fraction. This is because in an exclusive process, at least two gluons must be exchanged, rendering the process very sensitive to the target structure [1–3]. Additionally, measuring the total transverse momentum transfer provides access to the (event-by-event fluctuating) spatial distribution of the target nucleus at small momentum fraction $x_{\mathbb{P}}$ [4,5]. Finally, the probe is a photon whose structure is perturbative and its kinematics can be determined completely. Consequently, vector meson production will play a central role at the future Electron-Ion Collider [6] and Large Hadron-electron Collider/future circular collider in hadron-electron mode [7] nuclear deep inelastic scattering (DIS) facilities when looking for signals of gluon saturation.

Saturation effects are expected to be encountered in heavy nuclei at high energies where the parton densities become so large that gluon emission and gluon recombination balance each other. At such high densities, it is convenient to describe QCD dynamics using the color glass condensate (CGC) [8,9] effective theory. CGC calculations have been extensively applied across different collider experiments [10], yet unambiguous signatures of gluon saturation remain to be observed. Thus, it is important to focus on clean processes that are especially sensitive to saturation effects, such as exclusive vector meson production at the highest achievable energies [11]. Here, the J/ψ production process is intriguing, as the mass of the J/ψ is large enough to ensure perturbative stability, but low enough to keep the process sensitive to saturation.

Before the future $e + A$ colliders are realized, it is possible to study high-energy photoproduction processes in ultraperipheral collisions (UPCs) [4,12] at the Relativistic Heavy Ion Collider (RHIC) and the Large Hadron Collider (LHC); see, e.g., Refs. [13–15] for recent J/ψ production measurements. Although, in principle, one can access very small $x_{\mathbb{P}} \sim 10^{-5}$ at the LHC at forward rapidities, in ultraperipheral $\mathrm{Pb} + \mathrm{Pb} \to J/\psi + \mathrm{Pb} + \mathrm{Pb}$ there is a twofold ambiguity in the kinematics: J/ψ production at a given rapidity could result from a high-energy photon emitted from the first nucleus scattering off a small-$x_{\mathbb{P}}$ gluon from the other nucleus, or vice versa. Because the high-energy photon flux is heavily suppressed, the sensitivity to the very small-$x_{\mathbb{P}}$ structure is limited.

Recently the ALICE [16], CMS [14], and STAR [17,18] Collaborations extracted the center-of-mass-energy dependence of the $\gamma + A \to J/\psi + A$ cross section from

*heikki.mantysaari@jyu.fi

the measured J/ψ production cross section in UPCs using the method proposed in Ref. [19]. This made possible the study of photon-nucleus scattering at energies up to $W \sim 1$ TeV, enabling clean studies of gluon saturation in a unique kinematical domain.

J/ψ production in UPCs has been extensively studied within the CGC; see, e.g., Refs. [20–23]. The purpose of this article is to extend the UPC results presented in Ref. [21] to the high-energy photon-nucleus collisions covered by the recent photoproduction measurements. We present state-of-the-art CGC predictions for the energy dependence of the J/ψ photoproduction cross sections and nuclear suppression factors to determine the compatibility of the gluon saturation picture with the new data, providing access to very small $x_{\mathbb{P}}$. We also present a comparison to the new UPC measurement of the t-dependent incoherent cross section that has become available since the publication of Ref. [21].

Exclusive vector meson production in the color glass condensate. We calculate exclusive vector meson production using the same setup as in Ref. [21], which we briefly summarize here. At high energies, the process factorizes such that first the virtual photon fluctuates into a quark-antiquark dipole at leading order (see Refs. [24,25] for an extension to NLO), and then the quarks propagate eikonally through the target color field before forming a vector meson. As such, the coherent cross section for $\gamma + A \to J/\psi + A$ can be written as [5,26–28]

$$\frac{d\sigma^{\gamma A}}{dt} = \frac{1}{4\pi}|\langle \mathcal{A} \rangle_{x_{\mathbb{P}}}|^2, \tag{1}$$

and the incoherent cross section reads

$$\frac{d\sigma^{\gamma A}}{dt} = \frac{1}{4\pi}[\langle |\mathcal{A}|^2 \rangle_{x_{\mathbb{P}}} - |\langle \mathcal{A} \rangle_{x_{\mathbb{P}}}|^2]. \tag{2}$$

Here $\langle \rangle_{x_{\mathbb{P}}}$ refers to the average over target color field configurations at the given $x_{\mathbb{P}}$, and the scattering amplitude $\mathcal{A}$ is

$$-i\mathcal{A} = \int d^2\mathbf{r} d^2\mathbf{b} \int_0^1 \frac{dz}{4\pi} [\Psi_V^* \Psi_\gamma](Q^2, \mathbf{r}, z) \times e^{-i\mathbf{b}\cdot\boldsymbol{\Delta}} N(\mathbf{r}, \mathbf{b}, z). \tag{3}$$

In this work, we only consider photoproduction processes where $Q^2 = 0$.

All information about the target structure is encoded in the two-point Wilson line operator

$$N(\mathbf{r}, \mathbf{b}, z) = 1 - \frac{1}{N_c} \mathrm{tr}[V(\mathbf{b} + (1-z)\mathbf{r}) V^\dagger(\mathbf{b} - z\mathbf{r})]. \tag{4}$$

Here $\mathbf{r}$ and $\mathbf{b}$ are the dipole and impact parameter (center of the dipole) vectors, and the dependence on the longitudinal momentum fraction z takes into account the nonforward phase [29,30]. Explicit expressions for the photon and vector meson wave functions Ψ_γ and Ψ_V can be found from Ref. [31]. For the J/ψ we use the boosted Gaussian model with parameters constrained in Ref. [32]. The J/ψ wave function is not accurately known [33], but this uncertainty mostly affects the overall normalization and is to a large extent removed when the free parameters are constrained by the $\gamma + p \to J/\psi + p'$ data.

The Wilson lines at the initial $x_{\mathbb{P}} = 0.01$ are obtained from the McLerran-Venugopalan model [34,35]. The energy ($x_{\mathbb{P}}$) dependence is obtained by solving the Jalilian-Marian-Iancu-McLerran-Weigert-Leonidov-Kovner (JIMWLK) evolution equations [36]. The free parameters describing the proton saturation scale, scale of the coordinate space running coupling, and the fluctuating proton geometry are determined by fitting the J/ψ photoproduction cross section in $\gamma + p$ collisions as measured by H1 [37,38], ZEUS [39], ALICE [40,41] and LHCb [42,43] (see also Refs. [44–49]). These parameters are determined separately for the case where the proton has no substructure but only color charge fluctuations (referred to as "CGC" in this work), and for the case where the proton consists of three fluctuating hot spots ("CGC + shape fluct.").

When calculating cross sections for ultraperipheral collisions (Pb + Pb $\to J/\psi$ + Pb + Pb) the photon-nucleus cross section is multiplied by an equivalent photon flux as described in Ref. [21]. The UPC observables integrated over momentum transfer t considered in this work are not sensitive to the interference effect or to the nonzero but small photon transverse momentum, so these effects are not included here.

Results.

Vector meson photoproduction in UPCs: Before discussing photon-nucleus cross sections, we first compute coherent J/ψ production in ultraperipheral Pb + Pb collision. In this case there is no uncertainty related to the extraction of the photonuclear cross section, but sensitivity to the very small-$x_{\mathbb{P}}$ structure of the nucleus is limited.

The coherent J/ψ production cross section as a function of J/ψ rapidity is shown in Fig. 1. Because we use the same setup as in Ref. [21] summarized in Sec. II, the results are identical to those presented in our previous publication. Here we compare to newly available CMS data [14], covering a previously unexplored rapidity range, in addition to the most recent data from LHCb [15] and ALICE [13].

The inclusion of the new CMS dataset does not significantly modify the conclusions presented in Ref. [21]. The cross section is slightly smaller when proton shape fluctuations are included. This is because the nonlinear effects are stronger in the fluctuating case where there are regions with larger local saturation scales, leading to more suppression. The rapidity dependence of the ALICE, LHCb, and CMS data is quite well reproduced by our calculation

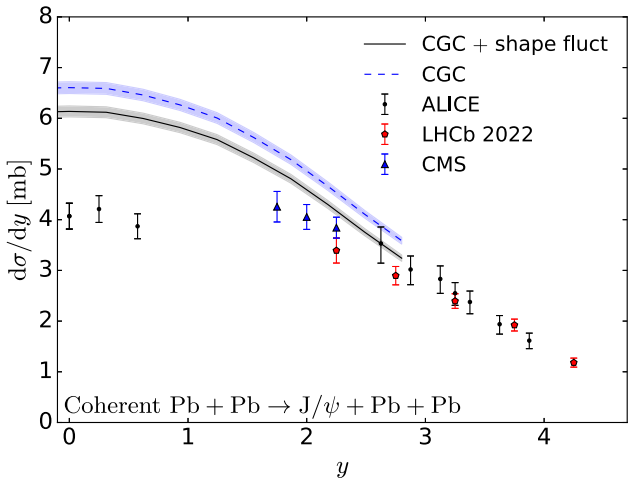

FIG. 1. Coherent J/ψ photoproduction cross section in ultraperipheral Pb + Pb collisions compared to the ALICE [13], CMS [14], and LHCb [15] data. The bands represent the statistical uncertainty of the calculation.

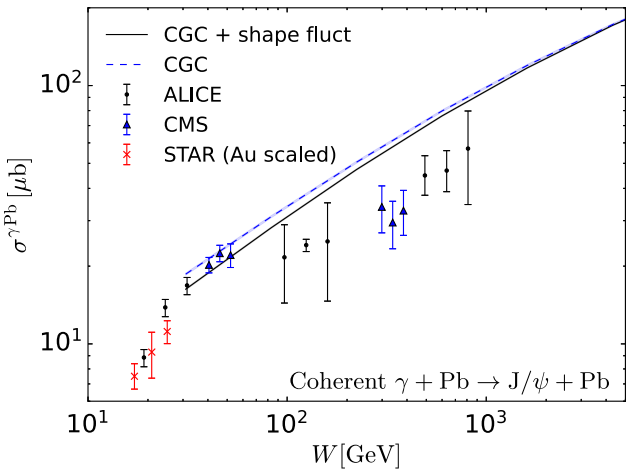

FIG. 2. Center-of-mass energy dependence of the coherent J/ψ photoproduction cross section compared to the ALICE [16], CMS [14], and scaled STAR [17,18] data.

in the $|y| \gtrsim 1.5$ region, but the ALICE midrapidity data are significantly overestimated.

Because of the twofold ambiguity of the UPC kinematics, at $y \neq 0$ one probes the nucleus at two different values of $x_{\mathbb{P}} = \frac{M_V}{\sqrt{s}} e^{\pm y}$, where M_V is the vector meson mass and $\sqrt{s}$ the nucleon-nucleon center-of-mass energy. The CGC calculations in Fig. 1 are limited to the region where $x_{\mathbb{P}} < 0.01$, as the initial condition for the JIMWLK evolution is parametrized at $x_{\mathbb{P}} = 0.01$. The larger-$x_{\mathbb{P}}$ contribution dominates in the large-y region, which means that our calculations agree with the LHC data well in the domain where the dominant contribution comes from the process with a relatively low photon-nucleon center-of-mass energy $W^2 = \sqrt{s} M_V e^{-y} \lesssim (60\ \text{GeV})^2$. Smaller $x_{\mathbb{P}}$ dominates at the lowest y values in this observable, implying that our calculation increasingly underestimates the nuclear suppression as $x_{\mathbb{P}}$ decreases.

Vector meson production in photon-nucleus collisions: We now move to the main focus of this article: energy dependent diffractive vector meson production in photon-nucleus collisions. The twofold ambiguity can be overcome and the photon-nucleus cross section extracted from the measured UPC cross section using the approach proposed in Ref. [19] based on measurements in different forward neutron multiplicity channels. This procedure has been recently employed by ALICE [16], CMS [14], and STAR [17,18] to measure the photoproduction cross section for the $\gamma + \text{Pb(Au)} \to J/\psi + \text{Pb(Au)}$ scattering.

The coherent J/ψ photoproduction cross section as a function of the photon-nucleon center-of-mass energy W is shown in Fig. 2. The results calculated for $\gamma + \text{Pb} \to J/\psi + \text{Pb}$, again with and without nucleon shape fluctuations, are compared to the available ALICE, CMS, and STAR data. The data point at $W = 125$ GeV with a very small uncertainty corresponds to midrapidity kinematics in UPCs at $\sqrt{s} = 5020$ GeV where there is no twofold ambiguity. The STAR measurements with gold targets are scaled to the photon-lead case by assuming an $A^{4/3}$ scaling [11].

The measured $\gamma + \text{Pb}$ cross section is well reproduced in the low center-of-mass energy $W \lesssim 100$ GeV region, but the high-energy cross sections are overestimated by up to 40%. This is consistent with the result in Fig. 1: The UPC cross section at forward rapidities where the low-W contribution dominates is well reproduced, but the midrapidity data corresponding to $W = 125$ GeV is overestimated by 50% (with nucleon shape fluctuations).

Although the normalization of the cross section is overestimated in the high-energy region, our calculations capture well the W dependence at $W \gtrsim 100$ GeV. The cross section for the case without proton shape fluctuations grows slightly more slowly as a function of energy compared to the case with proton substructure. This difference can be traced back to the fact that the parameter Λ_{QCD} controlling the running coupling scale in coordinate space determined in Ref. [21] is chosen to be smaller for the case using spherical nucleons, compared to the case where substructure fluctuations are included. This affects the evolution speed as a smaller Λ_{QCD} leads to a smaller α_s.

In order to quantify the magnitude of saturation effects in J/ψ photoproduction, we compute nuclear suppression factors separately for the coherent and incoherent channels. Following the definitions used in the recent experimental studies [14,16], we define the suppression factor for the coherent production as

$$S_{\text{coh}} = \sqrt{\frac{\sigma^{\gamma A}}{\sigma^{\text{IA}}}}. \tag{5}$$

Here

$$\sigma^{\mathrm{IA}} = \frac{\mathrm{d}\sigma^{\gamma p}}{\mathrm{d}t}(t=0)\int_{-t_{\mathrm{min}}} \mathrm{d}t|F(t)|^2 \tag{6}$$

is the corresponding cross section obtained from the impulse approximation [50,51], that is, the $\gamma + p$ result scaled to the $\gamma + \mathrm{Pb}$ case by only taking into account the nuclear form factor $F(t)$. In the LHC kinematics, we set $t_{\mathrm{min}} = 0$. We calculate the impulse approximation reference for the $\gamma + \mathrm{Pb}$ scattering exactly as the CMS Collaboration: We use the approximate nuclear form factor $F(t)$ from Ref. [52] with Woods-Saxon parameters $R_A = 6.62$ fm and $a = 0.535$ fm. When calculating S_{coh} for the gold nucleus to be compared with the STAR measurements, we use the same Hartree-Fock-Skyrme nuclear density profile as STAR used, e.g., in Ref. [51], which corresponds to $\int_{-t_{\mathrm{min}}} \mathrm{d}t|F(t)|^2 = 135.876\ \mathrm{GeV}^2$ [53].

We follow STAR [17,18] to define the nuclear modification factor for the incoherent cross section:

$$S_{\mathrm{incoh}} = \frac{\sigma^{\gamma+A\to \mathrm{J}/\psi+A^*}}{A(\sigma^{\gamma+p\to \mathrm{J}/\psi+p^*} + \sigma^{\gamma+p\to \mathrm{J}/\psi+p})}. \tag{7}$$

In general the incoherent cross section is expected to be more heavily suppressed: in the black disc limit where the fluctuations vanish, the incoherent $\gamma + A$ cross section vanishes unlike coherent production.

The obtained suppression factor for the coherent J/ψ photoproduction is shown in Fig. 3. Here we again show results calculated with and without nucleon substructure. The results are compared to the ALICE [16] and CMS [14] data. We obtain slightly more suppression than the observed $S_{\mathrm{coh}} \approx 0.9$ at the lowest center-of-mass energies $W \sim 45$ GeV, i.e., close to the initial condition of the JIMWLK evolution where the coherent photoproduction cross section was well reproduced as shown in Fig. 2. On the other hand, the suppression factor is overestimated for high center-of-mass energies. Consequently, the W dependence of the suppression factor is somewhat weaker in the employed CGC calculation compared to the LHC data. This feature is reflected above in the fact that both the $\gamma + \mathrm{Pb}$ cross section at high W and the UPC cross section at $y = 0$ (corresponding to $W = 125$ GeV) are overestimated, but lower-energy data is better reproduced. Note, however, that the impulse approximation baseline, Eq. (6), depends on the $\gamma + p \to \mathrm{J}/\psi + p$ cross section only at $t = 0$ and not on the t-integrated cross section, which is experimentally better constrained. Consequently, the reference calculated from our setup is not precisely constrained by HERA data and there is a corresponding model uncertainty in the obtained suppression factors S_{coh}. As seen in Fig. 1, when nucleon substructure fluctuations are included a stronger nuclear suppression (smaller cross section) is obtained. However, this effect is not visible in S_{coh} because the $\gamma + p \to \mathrm{J}/\psi + p$ references differ at $t = 0$ up to 10% although the t-integrated cross sections are identical as constrained in Ref. [21].

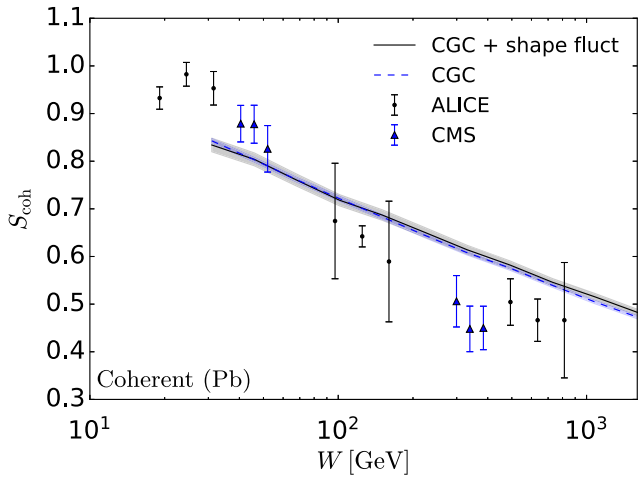

FIG. 3. Suppression factor for coherent production compared to the ALICE [16] and CMS data [14].

Comparisons to the STAR measurement of S_{coh} calculated using a gold target are shown in Table I. We calculate predictions at the initial condition of our JIMWLK evolution, $x_{\mathbb{P}} = 0.01$, which is smaller than $x_{\mathbb{P}} = 0.015$ probed in midrapidity measurements at STAR [17,18]. The JIMWLK evolution should not have a large effect in this small-$x_{\mathbb{P}}$ range, and we consider our predictions for S_{coh} to be relatively good approximations for STAR midrapidity kinematics. The STAR data are found to be compatible with our results. Furthermore, by separating the high-$x_{\mathbb{P}}$ and low-$x_{\mathbb{P}}$ contributions to the UPC cross section, STAR may also be able to measure the cross section at $x_{\mathbb{P}} = 0.01$.

We present the suppression factor for the incoherent photonuclear J/ψ production [Eq. (7)] in $\gamma + \mathrm{Pb}$ collisions as a function of W in Fig. 4. We compare to the STAR measurement in $\gamma + \mathrm{Au}$ collisions [17,18]. In order to use a $\gamma + p$ reference that is compatible with both the coherent and incoherent J/ψ production measurements at HERA, we include the proton shape fluctuations when calculating the denominator of Eq. (7) independently of whether the nucleon shape fluctuations are included in the nucleus.

TABLE I. Nuclear modification factors for J/ψ photoproduction in $\gamma + \mathrm{Au}$ collisions. The CGC predictions are calculated at $x_{\mathbb{P}} = 0.01$ and the STAR measurements are performed at $x_{\mathbb{P}} = 0.015$. The coherent suppression factors S_{coh} obtained with and without nucleon substructure fluctuations are compatible with each other within the numerical accuracy.

Channel	STAR [17,18]	CGC + shape fluct	CGC
S_{coh}	0.846 ± 0.063	0.89	0.90
S_{incoh}	$0.36^{+0.06}_{-0.07}$	0.58	0.32

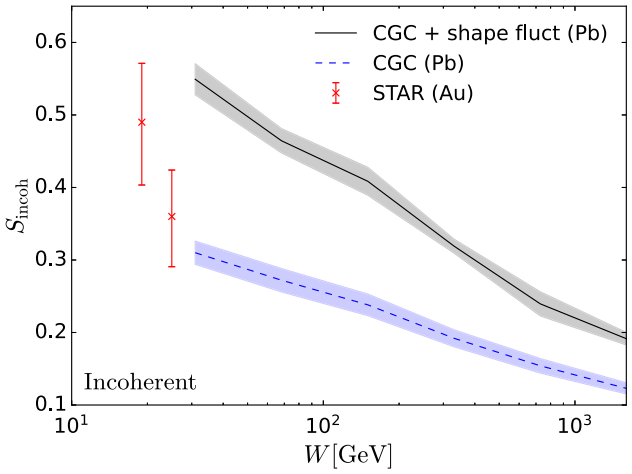

FIG. 4. Energy dependence of $S_{\rm incoh}$ as defined in (7) for Pb nuclei calculated from the CGC setup and compared to STAR data [17,18] for Au targets. The proton reference is always calculated with substructure fluctuations.

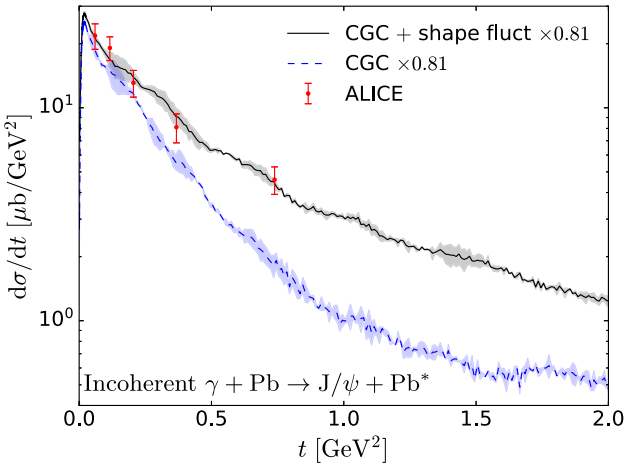

FIG. 5. Incoherent J/ψ production in $\gamma + {\rm Pb}$ collisions at midrapidity compared to the ALICE data [56].

Predictions for the $\gamma + {\rm Au}$ collisions in approximate STAR kinematics (calculated at $x_{\mathbb{P}} = 0.01$, compared to STAR data at $x_{\mathbb{P}} = 0.015$) are shown in Table I.

When nucleon shape fluctuations are included, the incoherent suppression factor is overestimated by ∼40% at low W in the STAR kinematics. This is qualitatively consistent with the fact that the incoherent cross section in UPCs [54] was found in Ref. [21] to be overestimated by ∼60% at midrapidity LHC kinematics at $\sqrt{s} = 2.76$ GeV. On the other hand, we note that in the W range close to the STAR kinematics, the obtained suppression factor for the coherent production is approximately compatible with the LHC data as shown in Fig. 3. If nucleon substructure fluctuations are not included for the nucleus, the suppression is overestimated. This is because substructure fluctuations at short distance scales enhance the incoherent cross section significantly in the high-$|t|$ region [21,55]. In our main setup with nucleon substructure included, we predict a faster W dependence for $S_{\rm incoh}$ compared to the $S_{\rm coh}$, a genuine feature that can be tested with future LHC data. The STAR data hints at an even faster center-of-mass energy dependence than that obtained in the setup with substructure fluctuations. The strong suppression at high energies for the incoherent case is a result of JIMWLK evolution generating a smoother nucleus with fewer fluctuations and eventually approaching the black disk limit.

Vector meson spectra: To complete the discussion about the implications of new experimental UPC and $\gamma + A$ data that have become available since the publication of Ref. [21], we calculate incoherent J/ψ production in $\gamma + {\rm Pb}$ collisions as a function of squared momentum transfer. The results shown in Fig. 5 are compared with the ALICE data at $W = 125$ GeV [56] corresponding to midrapidity kinematics in UPCs at $\sqrt{s} = 5020$ GeV. Based on Ref. [21] and the discussion above, we expect our incoherent cross section to overestimate the ALICE data. In order to better illustrate the shape of the t distribution (which is sensitive to the substructure fluctuations) relative to the ALICE data, we show the results normalized by a factor 0.81 determined by requiring that the ALICE data are optimally reproduced (χ^2 is minimized) with substructure fluctuations. Note that the (t-integrated) coherent cross section shown in Fig. 2 is overestimated by a slightly larger fraction. This hints at a small tension between the coherent and incoherent data, but firm conclusions will require a precise measurement of the t-integrated incoherent cross section at this energy.

Relying on the description of the slope alone, ALICE data prefer results with substructure fluctuations. Without such fluctuations, the calculated incoherent cross section decreases much faster in the $|t| \gtrsim 0.2$ GeV^2 region than the data. This is exactly the region where the t slope is significantly modified and controlled by the size of the nucleon constituents that fluctuate [21,55,57–59]. Similar conclusions supporting nucleon substructure fluctuations in nuclei based on comparisons to preliminary STAR data were reported in Ref. [21].

Conclusions. We have calculated J/ψ photoproduction cross sections in photon-nucleus collisions and the corresponding nuclear modification factors within the color glass condensate framework, where gluon saturation phenomena are naturally included. The experimentally measured coherent cross section is well described in the range $30\ {\rm GeV} < W < 50\ {\rm GeV}$ $(0.004 < x_{\mathbb{P}} < 0.01)$. At high $W \gtrsim 100$ GeV, we reproduce the center-of-mass energy dependence of the data but overestimate the overall normalization. This suggests that the experimental data would prefer even stronger saturation effects at very high energies than what is obtained from our setup which is constrained by the $\gamma + p \to {\rm J}/\psi + p$ data. This is also reflected by the fact that the nuclear suppression factor

obtained for the coherent cross section is larger than what is seen in the ALICE and CMS data at high energies, and has a weaker dependence on the center-of-mass energy.

The nuclear suppression factor for incoherent J/ψ photoproduction is highly sensitive to nucleon substructure fluctuations in heavy nuclei. The only measurement available from STAR at low W does not clearly prefer either a calculation with or without nucleon substructure fluctuations, leaving room for potential nuclear modification to the nucleon substructure within a heavy nucleus. The first data for the t dependence of the incoherent J/ψ production from LHC are found to be compatible with no nuclear modification to the substructure fluctuations, although we again do not find large enough nuclear suppression. Future measurements for the energy dependence of the incoherent $\gamma + A \to J/\psi + A^*$ cross section will make it possible to determine how the nucleon substructure fluctuations are modified by the saturation effects in heavy nuclei at high energies.

In the future, it will be important to consistently propagate the model uncertainties from fits to HERA $\gamma + p$ data (see e.g. Refs. [44,60]) to the calculations of high-energy $\gamma + \mathrm{Pb}$ scattering. Similarly, uncertainties originating from the nonperturbative vector meson wave function could be estimated [33]. This would allow one to determine if the strong nuclear suppression observed at the LHC can be described simultaneously with the $\gamma + p$ data where only weak saturation effects are expected [61]. Furthermore, all ingredients of the calculation should be advanced to next-to-leading order (NLO) accuracy; see Refs. [24,25,62–70]. First estimates [71] indicated that the NLO corrections have only a small effect on the nuclear modification factor in exclusive vector meson production. However, recently it was found that nuclear modification in inclusive particle production in proton-nucleus collisions depends strongly on the initial condition chosen for the small-x evolution [72], despite the fact that all these initial conditions have been constrained by the same proton structure function data [64]. As such, the NLO effect on the nuclear modification factor studied in this work is currently unknown. We emphasize that in the applied CGC setup there are no free parameters when moving from proton to nucleus and consequently the obtained nuclear suppression factor is a genuine prediction based on gluon saturation. This is in contrast to approaches based on collinear factorization where the nuclear modification to the (generalized) parton distribution function (PDF) is fit to data. Using nuclear PDFs determined from global analyses, it is possible to get a good description of the nuclear suppression observed in UPCs [2,3]. Such global analyses including HERA and UPC data could also be performed within the CGC framework. If good agreement with data is achieved this method could provide powerful constraints on saturation effects in heavy nuclei.

Acknowledgments. We thank Z. Tu and Z. Ye for clarifying details of the STAR and CMS data and V. Guzey for useful discussions. H. M. is supported by the Research Council of Finland, the Centre of Excellence in Quark Matter, and Projects No. 338263 and No. 346567, and under the European Union's Horizon 2020 research and innovation programme by the European Research Council (ERC, Grant Agreement No. ERC-2018-ADG-835105 YoctoLHC) and by the STRONG-2020 project (Grant Agreement No. 824093) and wishes to thank the Electron-Ion Collider Theory Institute at BNL for its hospitality during the completion of this work. B. P. S. is supported by the U.S. Department of Energy, Office of Science, Office of Nuclear Physics, under DOE Contract No. DE-SC0012704 and within the framework of the Saturated Glue (SURGE) Topical Theory Collaboration. F. S. is supported in part by DOE under Contract No. DE-AC02-05CH11231, by NSF under Grant No. OAC-2004571 within the X-SCAPE Collaboration, and the INT's U.S. DOE under Grant No. DE-FG02-00ER41132. Computing resources from CSC–IT Center for Science in Espoo, Finland and the Finnish Grid and Cloud Infrastructure (persistent identifier urn:nbn:fi:research-infras-2016072533) were used in this work.

The content of this article does not reflect the official opinion of the European Union and responsibility for the information and views expressed therein lies entirely with the authors.

[1] S. J. Brodsky, L. Frankfurt, J. F. Gunion, A. H. Mueller, and M. Strikman, Diffractive leptoproduction of vector mesons in QCD, Phys. Rev. D **50**, 3134 (1994).

[2] V. Guzey, E. Kryshen, M. Strikman, and M. Zhalov, Nuclear suppression from coherent J/ψ photoproduction at the Large Hadron Collider, Phys. Lett. B **816**, 136202 (2021).

[3] K. J. Eskola, C. A. Flett, V. Guzey, T. Löytäinen, and H. Paukkunen, Next-to-leading order perturbative QCD predictions for exclusive J/ψ photoproduction in oxygen-oxygen and lead-lead collisions at energies available at the CERN Large Hadron Collider, Phys. Rev. C **107**, 044912 (2023).

[4] S. R. Klein and H. Mäntysaari, Imaging the nucleus with high-energy photons, Nat. Rev. Phys. **1**, 662 (2019).

[5] H. Mäntysaari, Review of proton and nuclear shape fluctuations at high energy, Rep. Prog. Phys. **83**, 082201 (2020).

[6] R. Abdul Khalek *et al.*, Science requirements and detector concepts for the electron-ion collider: EIC Yellow report, Nucl. Phys. **A1026**, 122447 (2022).
[7] P. Agostini *et al.* (LHeC and FCC-he Study Group Collaborations), The large hadron-electron collider at the HL-LHC, J. Phys. G **48**, 110501 (2021).
[8] F. Gelis, E. Iancu, J. Jalilian-Marian, and R. Venugopalan, The color glass condensate, Annu. Rev. Nucl. Part. Sci. **60**, 463 (2010).
[9] Y. V. Kovchegov and E. Levin, *Quantum Chromodynamics at High Energy* (Oxford University Press, New York, 2013), Vol. 33.
[10] A. Morreale and F. Salazar, Mining for gluon saturation at colliders, Universe **7**, 312 (2021).
[11] H. Mäntysaari and R. Venugopalan, Systematics of strong nuclear amplification of gluon saturation from exclusive vector meson production in high energy electron–nucleus collisions, Phys. Lett. B **781**, 664 (2018).
[12] C. A. Bertulani, S. R. Klein, and J. Nystrand, Physics of ultra-peripheral nuclear collisions, Annu. Rev. Nucl. Part. Sci. **55**, 271 (2005).
[13] S. Acharya *et al.* (ALICE Collaboration), Coherent J/ψ and ψ' photoproduction at midrapidity in ultra-peripheral Pb-Pb collisions at $\sqrt{s_{\rm NN}} = 5.02$ TeV, Eur. Phys. J. C **81**, 712 (2021).
[14] A. Tumasyan *et al.* (CMS Collaboration), Probing small Bjorken-x nuclear gluonic structure via coherent J/ψ photoproduction in ultraperipheral Pb-Pb collisions at $\sqrt{s_{NN}} = 5.02$ TeV, Phys. Rev. Lett. **131**, 262301 (2023).
[15] R. Aaij *et al.* (LHCb Collaboration), Study of exclusive photoproduction of charmonium in ultra-peripheral lead-lead collisions, J. High Energy Phys. 06 (2023) 146.
[16] S. Acharya *et al.* (ALICE Collaboration), Energy dependence of coherent photonuclear production of J/ψ mesons in ultra-peripheral Pb-Pb collisions at $\sqrt{s_{\rm NN}} = 5.02$ TeV, J. High Energy Phys. 10 (2023) 119.
[17] STAR Collaboration, Exclusive J/ψ, $\psi(2s)$, and e^+e^- pair production in Au + Au ultra-peripheral collisions at RHIC, arXiv:2311.13632.
[18] STAR Collaboration, Observation of strong nuclear suppression in exclusive J/ψ photoproduction in Au + Au ultra-peripheral collisions at RHIC, arXiv:2311.13637.
[19] V. Guzey, M. Strikman, and M. Zhalov, Disentangling coherent and incoherent quasielastic J/ψ photoproduction on nuclei by neutron tagging in ultraperipheral ion collisions at the LHC, Eur. Phys. J. C **74**, 2942 (2014).
[20] T. Lappi and H. Mantysaari, J/ψ production in ultraperipheral Pb + Pb and p + Pb collisions at energies available at the CERN Large Hadron Collider, Phys. Rev. C **87**, 032201 (2013).
[21] H. Mäntysaari, F. Salazar, and B. Schenke, Nuclear geometry at high energy from exclusive vector meson production, Phys. Rev. D **106**, 074019 (2022).
[22] V. P. Gonçalves, M. V. T. Machado, B. D. Moreira, F. S. Navarra, and G. S. dos Santos, Color dipole predictions for the exclusive vector meson photoproduction in pp, pPb, and PbPb collisions at run 2 LHC energies, Phys. Rev. D **96**, 094027 (2017).
[23] D. Bendova, J. Cepila, J. G. Contreras, and M. Matas, Photonuclear J/ψ production at the LHC: Proton-based versus nuclear dipole scattering amplitudes, Phys. Lett. B **817**, 136306 (2021).
[24] H. Mäntysaari and J. Penttala, Exclusive heavy vector meson production at next-to-leading order in the dipole picture, Phys. Lett. B **823**, 136723 (2021).
[25] H. Mäntysaari and J. Penttala, Complete calculation of exclusive heavy vector meson production at next-to-leading order in the dipole picture, J. High Energy Phys. 08 (2022) 247.
[26] M. L. Good and W. D. Walker, Diffraction dissociation of beam particles, Phys. Rev. **120**, 1857 (1960).
[27] H. I. Miettinen and J. Pumplin, Diffraction scattering and the parton structure of hadrons, Phys. Rev. D **18**, 1696 (1978).
[28] A. Caldwell and H. Kowalski, Investigating the gluonic structure of nuclei via J/ψ scattering, Phys. Rev. C **81**, 025203 (2010).
[29] Y. Hatta, B.-W. Xiao, and F. Yuan, Gluon tomography from deeply virtual Compton scattering at small-x, Phys. Rev. D **95**, 114026 (2017).
[30] H. Mäntysaari, K. Roy, F. Salazar, and B. Schenke, Gluon imaging using azimuthal correlations in diffractive scattering at the electron-ion collider, Phys. Rev. D **103**, 094026 (2021).
[31] H. Kowalski, L. Motyka, and G. Watt, Exclusive diffractive processes at HERA within the dipole picture, Phys. Rev. D **74**, 074016 (2006).
[32] H. Mäntysaari and P. Zurita, In depth analysis of the combined HERA data in the dipole models with and without saturation, Phys. Rev. D **98**, 036002 (2018).
[33] T. Lappi, H. Mäntysaari, and J. Penttala, Relativistic corrections to the vector meson light front wave function, Phys. Rev. D **102**, 054020 (2020).
[34] L. D. McLerran and R. Venugopalan, Computing quark and gluon distribution functions for very large nuclei, Phys. Rev. D **49**, 2233 (1994).
[35] L. D. McLerran and R. Venugopalan, Gluon distribution functions for very large nuclei at small transverse momentum, Phys. Rev. D **49**, 3352 (1994).
[36] A. H. Mueller, A simple derivation of the JIMWLK equation, Phys. Lett. B **523**, 243 (2001).
[37] H1 Collaboration, Elastic J/ψ production at HERA, Eur. Phys. J. C **46**, 585 (2006).
[38] C. Alexa *et al.* (H1 Collaboration), Elastic and proton-dissociative photoproduction of J/ψ mesons at HERA, Eur. Phys. J. C **73**, 2466 (2013).
[39] S. Chekanov *et al.* (ZEUS Collaboration), Exclusive photoproduction of J/ψ mesons at HERA, Eur. Phys. J. C **24**, 345 (2002).
[40] B. B. Abelev *et al.* (ALICE Collaboration), Exclusive J/ψ photoproduction off protons in ultra-peripheral p-Pb collisions at $\sqrt{s_{\rm NN}} = 5.02$ TeV, Phys. Rev. Lett. **113**, 232504 (2014).
[41] S. Acharya *et al.* (ALICE Collaboration), Energy dependence of exclusive J/ψ photoproduction off protons in ultra-peripheral p–Pb collisions at $\sqrt{s_{\rm NN}} = 5.02$ TeV, Eur. Phys. J. C **79**, 402 (2019).
[42] R. Aaij *et al.* (LHCb Collaboration), Updated measurements of exclusive J/ψ and $\psi(2S)$ production cross-sections in pp collisions at $\sqrt{s} = 7$ TeV, J. Phys. G **41**, 055002 (2014).

[43] R. Aaij *et al.* (LHCb Collaboration), Central exclusive production of J/ψ and $\psi(2S)$ mesons in pp collisions at $\sqrt{s} = 13$ TeV, J. High Energy Phys. 10 (2018) 167.
[44] H. Mäntysaari, B. Schenke, C. Shen, and W. Zhao, Bayesian inference of the fluctuating proton shape, Phys. Lett. B **833**, 137348 (2022).
[45] H. Mäntysaari and B. Schenke, Revealing proton shape fluctuations with incoherent diffraction at high energy, Phys. Rev. D **94**, 034042 (2016).
[46] H. Mäntysaari and B. Schenke, Evidence of strong proton shape fluctuations from incoherent diffraction, Phys. Rev. Lett. **117**, 052301 (2016).
[47] H. Mäntysaari and B. Schenke, Confronting impact parameter dependent JIMWLK evolution with HERA data, Phys. Rev. D **98**, 034013 (2018).
[48] A. Kumar and T. Toll, Investigating the structure of gluon fluctuations in the proton with incoherent diffraction at HERA, Eur. Phys. J. C **82**, 837 (2022).
[49] J. Cepila, J. G. Contreras, and J. D. Tapia Takaki, Energy dependence of dissociative J/ψ photoproduction as a signature of gluon saturation at the LHC, Phys. Lett. B **766**, 186 (2017).
[50] G. F. Chew and G. C. Wick, The impulse approximation, Phys. Rev. **85**, 636 (1952).
[51] V. Guzey, E. Kryshen, M. Strikman, and M. Zhalov, Evidence for nuclear gluon shadowing from the ALICE measurements of PbPb ultraperipheral exclusive J/ψ production, Phys. Lett. B **726**, 290 (2013).
[52] S. Klein and J. Nystrand, Exclusive vector meson production in relativistic heavy ion collisions, Phys. Rev. C **60**, 014903 (1999).
[53] Z. Tu (private communication).
[54] E. Abbas *et al.* (ALICE Collaboration), Charmonium and e^+e^- pair photoproduction at mid-rapidity in ultra-peripheral Pb-Pb collisions at $\sqrt{s_{\rm NN}} = 2.76$ TeV, Eur. Phys. J. C **73**, 2617 (2013).
[55] H. Mäntysaari and B. Schenke, Probing subnucleon scale fluctuations in ultraperipheral heavy ion collisions, Phys. Lett. B **772**, 832 (2017).
[56] S. Acharya *et al.* (ALICE Collaboration), First measurement of the $|t|$-dependence of incoherent J/ψ photonuclear production, arXiv:2305.06169.
[57] T. Lappi and H. Mantysaari, Incoherent diffractive J/ψ-production in high energy nuclear DIS, Phys. Rev. C **83**, 065202 (2011).
[58] S. Demirci, T. Lappi, and S. Schlichting, Proton hot spots and exclusive vector meson production, Phys. Rev. D **106**, 074025 (2022).
[59] T. Toll, Subnucleon fluctuations in coherent and incoherent ultra-peripheral AA collisions at LHC and RHIC with the Sartre event generator, SciPost Phys. Proc. **8**, 148 (2022).
[60] C. Casuga, M. Karhunen, and H. Mäntysaari, Inferring the initial condition for the Balitsky-Kovchegov equation, Phys. Rev. D **109**, 054018 (2024).
[61] N. Armesto, T. Lappi, H. Mäntysaari, H. Paukkunen, and M. Tevio, Signatures of gluon saturation from structure-function measurements, Phys. Rev. D **105**, 114017 (2022).
[62] I. Balitsky and G. A. Chirilli, Rapidity evolution of Wilson lines at the next-to-leading order, Phys. Rev. D **88**, 111501 (2013).
[63] A. Kovner, M. Lublinsky, and Y. Mulian, Jalilian-Marian, Iancu, McLerran, Weigert, Leonidov, Kovner evolution at next to leading order, Phys. Rev. D **89**, 061704 (2014).
[64] G. Beuf, H. Hänninen, T. Lappi, and H. Mäntysaari, Color glass condensate at next-to-leading order meets HERA data, Phys. Rev. D **102**, 074028 (2020).
[65] D. Bendova, J. Cepila, J. G. Contreras, t. V. P. Gonçalves, and M. Matas, Diffractive deeply inelastic scattering in future electron-ion colliders, Eur. Phys. J. C **81**, 211 (2021).
[66] E. Iancu, J. D. Madrigal, A. H. Mueller, G. Soyez, and D. N. Triantafyllopoulos, Resumming double logarithms in the QCD evolution of color dipoles, Phys. Lett. B **744**, 293 (2015).
[67] B. Ducloué, E. Iancu, A. H. Mueller, G. Soyez, and D. N. Triantafyllopoulos, Non-linear evolution in QCD at high-energy beyond leading order, J. High Energy Phys. 04 (2019) 081.
[68] G. Beuf, Improving the kinematics for low-x QCD evolution equations in coordinate space, Phys. Rev. D **89**, 074039 (2014).
[69] H. Hänninen, H. Mäntysaari, R. Paatelainen, and J. Penttala, Proton structure functions at next-to-leading order in the dipole picture with massive quarks, Phys. Rev. Lett. **130**, 192301 (2023).
[70] P. Caucal, F. Salazar, B. Schenke, T. Stebel, and R. Venugopalan, Back-to-back inclusive dijets in DIS at small x: Complete NLO results and predictions, Phys. Rev. Lett. **132**, 081902 (2024).
[71] T. Lappi, H. Mäntysaari, and J. Penttala, Higher-order corrections to exclusive heavy vector meson production, SciPost Phys. Proc. **8**, 133 (2022).
[72] H. Mäntysaari and Y. Tawabutr, Complete next-to-leading order calculation of single inclusive π^0 production in forward proton-nucleus collisions, Phys. Rev. D **109**, 034018 (2024).